

cortices in one', with twice the number of neurons underneath a square millimetre of surface than the remainder of neocortex<sup>12</sup>. The density of neurons in the rest of neocortex scales similarly as in V1 (ref. 12), and all of the hominoid thalamic nuclei also have neuronal densities that vary in about the same way as in LGN<sup>13–15</sup>; altogether, then, the relations between number of thalamic neurons and number of neocortical neurons is about the same as the 3/2 power scaling law described above for the primary visual cortex.

The conservation of these scaling relations raises the possibility that a similar basis for the scaling laws exists for all cortical areas. In this view, each cortical area would be provided with a map of some sort—perhaps one with very abstract quantities—and the job of the cortex would be to extract some characteristic of the map at each point that would be represented as a location code by the neurons in each map 'pixel'. Note that the information in the map need not be supplied by thalamus; this structure would only have to determine the number of pixels in the map. If  $n$  pixels are present in a cortical region, then the number of neurons per pixel needed to maintain the same resolution within a pixel as across pixels would vary as  $n^{1/2}$ . A 3/2 power relation would result. □

**Methods**

To obtain the relation between the number of LGN and V1 neurons, I must make use of three separately determined scaling relations. First, for haplorhines, the volume  $V$  of the grey matter in V1 is related to the LGN volume  $v$  by a power law<sup>4,16</sup> (see Fig. 2),

$$V = Av^\alpha$$

where  $A = 14.61 \pm 4.78$  and  $\alpha = 1.125 \pm 0.057$ ; volumes are measured in cubic millimetres and refer to both hemispheres.

These volumes can be converted to numbers of neurons, if the neuronal densities in LGN and V1 are known. The numbers of neurons  $n$  in the LGN, as a function of LGN volume  $v$ , conform to a power law<sup>17</sup> for 23 haplorhines and 17 strepsirhines,

$$n = Bv^\beta$$

with  $\beta = 0.659 \pm 0.06$  for haplorhines and  $\beta = 0.683 \pm 0.22$  for the strepsirhines, values that are not significantly different. The scale factor  $B$ , however, is different with a value of  $0.071 \pm 0.025$  for haplorhines and  $0.046 \pm 0.029$  for strepsirhines. This power law is based on data from ref. 17 combined with data from ref. 4.

The relation between V1 volume  $V$  and the number of V1 neurons  $N$  also follows the power law,

$$N = DV^\delta$$

where  $D = 0.232$  and  $\delta = 0.902$ . This relation is obtained by using the observation<sup>12</sup> that 0.195 million neurons are found beneath a square millimetre of V1 surface in primates (the value is corrected for 18% shrinkage), and the weak power law dependence of V1 thickness  $t$  on cortical surface area  $S$  described<sup>12,18</sup> by;

$$t = 0.825S^{0.108}$$

When  $V$  and  $v$  are converted to  $N$  and  $n$  with the equations above, a power law results (Fig. 1) with an exponent  $\lambda$ :

$$\lambda = \alpha\delta/\beta = 1.54 \pm 0.072$$

Received 7 December 2000; accepted 31 January 2001.

1. Finlay, B. L. & Darlington, R. B. Linked regularities in the development and evolution of mammalian brains. *Science* **268**, 1578–1584 (1995).
2. Barton, R. A. & Harvey, P. H. Mosaic evolution of brain structure in mammals. *Nature* **405**, 1055–1058 (2000).
3. Andrews, T. J., Halpern, S. D. & Purves, D. Correlated size variations in human visual cortex, lateral geniculate nucleus, and optic tract. *J. Neurosci.* **17**, 2859–2868 (1997).
4. Stephan, H., Frahm, H. D. & Baron, G. New and revised data on volumes and brain structures in insectivores and primates. *Folia primatol.* **35**, 1–29 (1981).
5. Schein, S. J. & de Monasterio, F. M. Mapping of retinal and geniculate neurons onto striate cortex of macaque. *J. Neurosci.* **7**, 996–1009 (1987).
6. Ahmad, A. & Spear, P. D. Effects of aging on the size, density, and number of rhesus monkey lateral geniculate neurons. *J. Comp. Neurol.* **334**, 631–643 (1993).
7. Hubel, D. H. & Wiesel, T. N. Receptive fields and functional architecture of monkey striate cortex. *J. Physiol. (Lond.)* **195**, 215–243 (1968).
8. Bonhoeffer, T. & Grinvald, A. Iso-orientation domains in cat visual cortex are arranged in pinwheel-like patterns. *Nature* **353**, 429–431 (1991).
9. Swindale, N. V. How many maps are there in visual cortex? *Cereb. Cortex* **10**, 633–643 (2000).
10. Issa, N. P., Trepel, C. & Stryker, M. P. Spatial frequency maps in cat visual cortex. *J. Neurosci.* **20**, 8504–8514 (2000).
11. Frahm, H. D., Stephan, H. & Stephan, M. Comparison of brain structure volumes in Insectivora and Primates. I. Neocortex. *J. Hirnforsch.* **23**, 375–389 (1982).

12. Rockel, A. J., Hiorns, R. W. & Powell, T. P. The basic uniformity in structure of the neocortex. *Brain* **103**, 221–244 (1980).
13. Armstrong, E. A quantitative comparison of the hominoid thalamus. IV. Posterior association nuclei—the pulvinar and lateral posterior nucleus. *Am. J. Phys. Anthropol.* **55**, 369–383 (1981).
14. Armstrong, E. A quantitative comparison of the hominoid thalamus: II. Limbic nuclei anterior principalis and lateralis dorsalis. *Am. J. Phys. Anthropol.* **52**, 43–54 (1980).
15. Armstrong, E. Quantitative comparison of the hominoid thalamus. I. Specific sensory relay nuclei. *Am. J. Phys. Anthropol.* **51**, 365–382 (1979).
16. Frahm, H. D., Stephan, H. & Baron, G. Comparison of brain structure volumes in insectivora and primates. V. Area striata (AS). *J. Hirnforsch.* **25**, 537–557 (1984).
17. Shulz, H.-D. *Metrische Untersuchungen an den Schichten des Corpus Geniculatum Laterale tag- und Nachtaktiven Primaten*. Thesis, Johann Wolfgang Goethe-Universität Frankfurt (1967).
18. Fritschy, J. M. & Garey, L. J. Quantitative changes in morphological parameters in the developing visual cortex of the marmoset monkey. *Brain Res.* **394**, 173–888 (1986).

**Acknowledgements**

Much of the work described here was done at the Santa Fe Institute and the Aspen Center for Physics, and I thank those institutions for their support. I also thank T. Albright, S. Gandhi and I. Brivanlou for comments on an earlier draft.

Correspondence and requests for materials should be addressed to the author (e-mail: cfs@salk.edu).

.....  
**Interocular rivalry revealed in the human cortical blind-spot representation**

**Frank Tong\* & Stephen A. Engel†**

\* Department of Psychology, Princeton University, Princeton, New Jersey 08544, USA  
 † Department of Psychology, University of California Los Angeles, Los Angeles, California 90095, USA

.....  
**To understand conscious vision, scientists must elucidate how the brain selects specific visual signals for awareness. When different monocular patterns are presented to the two eyes, they rival for conscious expression such that only one monocular image is perceived at a time<sup>1,2</sup>. Controversy surrounds whether this binocular rivalry reflects neural competition among pattern representations or monocular channels<sup>3,4</sup>. Here we show that rivalry arises from interocular competition, using functional magnetic resonance imaging of activity in a monocular region of primary visual cortex corresponding to the blind spot. This cortical region greatly prefers stimulation of the ipsilateral eye to that of the blind-spot eye. Subjects reported their dominant percept while viewing rivalrous orthogonal gratings in the visual location corresponding to the blind spot and its surround. As predicted by interocular rivalry, the monocular blind-spot representation was activated when the ipsilateral grating became perceptually dominant and suppressed when the blind-spot grating became dominant. These responses were as large as those observed during actual alternations between the gratings, indicating that rivalry may be fully resolved in monocular visual cortex. Our findings provide the first physiological evidence, to our knowledge, that interocular competition mediates binocular rivalry, and indicate that V1 may be important in the selection and expression of conscious visual information.**

Despite extensive research, the neural basis of binocular rivalry has remained highly controversial. Specifically, it is debated whether discrepant monocular patterns rival because of interocular competition or pattern competition. Human psychophysical studies have provided evidence that rivalry results from interocular competition among monocular neurons in primary visual cortex (V1)<sup>3</sup>. However, single-unit recordings in awake, behaving monkeys have

yielded negligible evidence of rivalry-related activity in V1, inconsistent effects in visual areas V4 and MT, and strong effects in inferotemporal cortex<sup>4-6</sup>. These neurophysiological findings instead indicate that rivalry may result from competition among incompatible pattern representations at higher levels of the visual pathway, well after inputs from the two eyes have converged in V1.

To resolve this issue, we used functional magnetic resonance imaging (fMRI) to monitor rivalry-related activity in a monocular region of human V1 corresponding to the blind spot. The blind spot is a part of the retina that has no photoreceptors; its size is around  $4 \times 6^\circ$  and it is about  $15^\circ$  medial to the fovea (Fig. 1a). In human primary visual cortex, the blind spot is represented as a relatively large monocular region (around  $10 \text{ mm} \times 5 \text{ mm}$ ; J. C. Horton, personal communication) that receives direct input solely from the ipsilateral eye and not from the (contralateral)

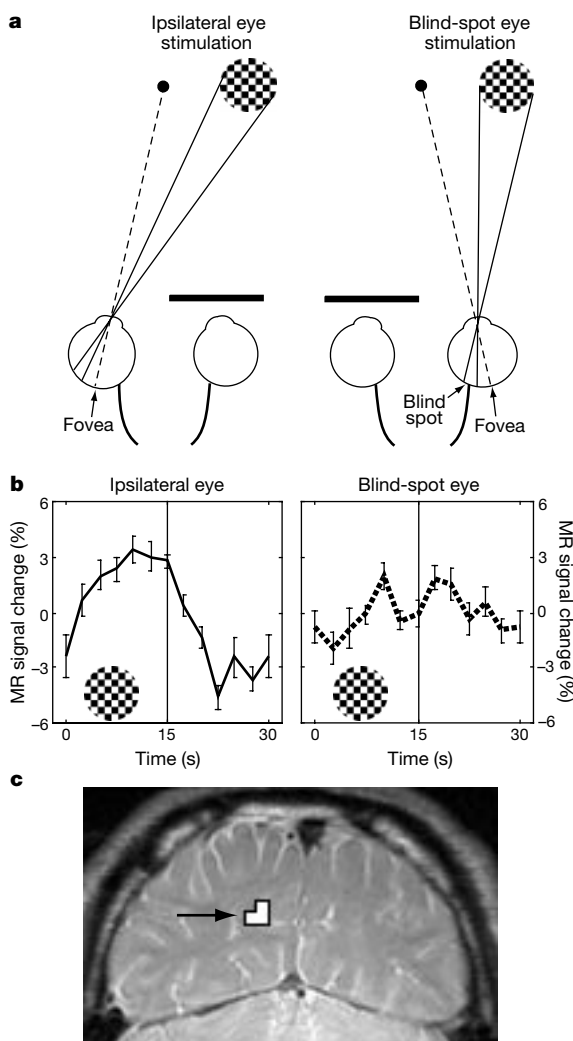


**Figure 1** Localization of the V1 blind-spot representation. **a**, Viewing conditions. Subjects maintained fixation on a reference point while viewing a flickering checkerboard pattern (stimulus size  $8^\circ$ , check size  $1^\circ$ , temporal frequency 7.5 Hz, contrast 100%) with either the ipsilateral eye or blind-spot eye. The centre of the checkerboard fell on the blind spot (optic nerve head, size  $\sim 4^\circ \times 6^\circ$ ) of the right eye but not the left eye. **b**, Average fMRI responses in the V1 blind-spot representation of one subject during stimulation of the ipsilateral or blind-spot eye. Data represent mean  $\pm$  s.e. of eight stimulus periods (on 15 s, off 15 s) and are expressed in per cent signal change relative to the mean MR level throughout the scan. This region is activated by ipsilateral stimulation only. **c**, V1 representation of the right eye's blind spot in the left calcarine sulcus (three voxels highlighted in white, voxel size  $3.1 \times 3.1 \times 4 \text{ mm}$ , slice plane perpendicular to calcarine). Functional data are superimposed on high-resolution anatomical T2-weighted images.

blind-spot eye. The monocular V1 blind-spot representation is large enough for functional imaging<sup>7</sup>.

Functional MRI has sufficient sensitivity and temporal resolution to detect rivalry-related responses in stimulus-selective extrastriate areas<sup>8</sup>. We predicted that if rivalry arises from interocular competition, then the ipsilateral-responsive neurons in the V1 blind-spot representation should show increased activity when subjects perceive a grating pattern presented to the ipsilateral eye and suppressed activity when subjects perceive a rivalrous grating presented to the blind-spot eye. Such excitation and suppression should occur even though both gratings are constantly present. Furthermore, if rivalry is fully resolved through interocular competition, then these neural responses during rivalry should be identical to those evoked by actual stimulus alternations between the ipsilateral grating and the blind-spot grating.

We performed three types of fMRI scan: V1 blind-spot localization scans, rivalry scans and stimulus alternation scans. Before MRI scanning, subjects mapped the visual field location of the right eye's blind spot by manipulating the location and size of a black flickering circular probe. During V1 blind-spot localization scans, subjects maintained fixation while viewing on/off sequences of a flickering checkerboard pattern using either their left ipsilateral eye or right blind-spot eye (Fig. 1a). The checkerboard was presented in the region of visual space corresponding to the blind spot and its immediate surround with a diameter of  $8^\circ$ , almost twice the size of the blind spot. Although the blind spot could not register the central portion of the checkerboard, the stimulus was perceptually filled in owing to stimulation of the blind spot's surround<sup>9</sup>.

The V1 blind-spot representation was reliably identified on the basis of the voxels in the left calcarine sulcus that showed a greater response to stimulation of the ipsilateral eye than of the blind-spot eye (see Methods). Figure 1 shows the fMRI response and anatomical locus of this region in one subject. The V1 blind-spot representation was highly monocular, responding vigorously to stimulation of the ipsilateral eye (Fig. 1b, left) and negligibly to stimulation of the blind-spot eye (Fig. 1b, right). In all subjects, this monocular region was located in the depth of the calcarine sulcus (Fig. 1c), a location that is always contained within primary visual cortex<sup>10</sup>.

During rivalry scans, a red vertical grating was presented to one eye and a green horizontal grating was presented to the other eye in the visual location corresponding to the blind spot and its surround

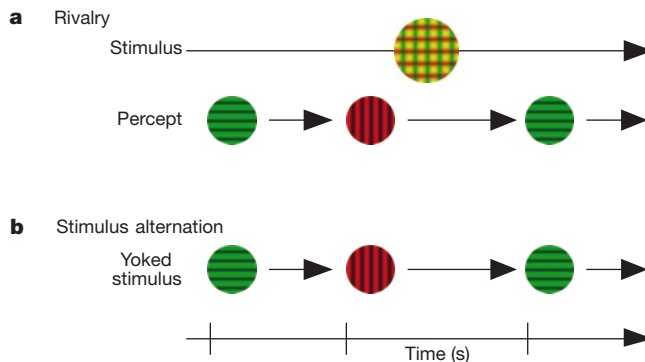


**Figure 2** Binocular rivalry and stimulus alternation tasks. **a**, Rivalrous oscillating sine-wave gratings were presented to the blind-spot eye and ipsilateral eye (size  $8^\circ$ ). When viewed through red and green filter glasses, only the green horizontal grating could be seen through one eye and only the red vertical grating through the other eye (spatial frequency 0.67 cycles per degree, speed 2 Hz, direction reversal every 500 ms, contrast 75%, mean luminance through matching filter  $3.4 \text{ cd m}^{-2}$ ). Although both gratings were constantly present, subjects reported alternately perceiving either the red or green grating. **b**, On stimulus alternation scans, the physical stimulus alternated between the red grating and green grating using the sequence of reported alternations from a previous rivalry scan. Subjects reported when the stimulus changed to the red or green grating.

(Fig. 2a). Gratings moved back and forth within a stationary circular aperture to ensure continuous visual stimulation. Subjects used a button box to report whenever their dominant percept changed to the vertical grating or horizontal grating, or if a blend of the two gratings persisted.

On subsequent stimulus alternation scans, the physical stimulus alternated between non-rivalrous monocular presentations of either the red vertical grating or the green horizontal grating using the same sequence of alternations reported in a previous rivalry scan (Fig. 2b). To mimic the phenomenal alternations of rivalry, one monocular stimulus would gradually fade from maximum to zero contrast while the other monocular grating would gradually appear (zero to maximum contrast) over 250 ms. Subjects were instructed to report when the stimulus switched to the vertical grating, horizontal grating or a blend of the two stimuli.

Subjects reported normal rivalry alternations between the ipsilateral and blind-spot gratings with extensive periods of exclusive dominance and minimal perceptual blending (Table 1). The ability of the blind-spot surrounding grating to suppress the entire ipsilateral grating, including its central 'unpaired' region, is consistent with the finding that binocular rivalry can occur among nonoverlapping stimuli<sup>2</sup>. In separate psychophysical studies, we have confirmed the rivalrous nature of these interactions encompassing the blind spot—increasing the contrast of either grating decreased the dominance duration of the opposing grating, as is found in foveal vision<sup>11</sup>.

Three out of four subjects showed significantly longer dominance durations for the ipsilateral grating than for the blind-spot grating

(S1, S2, S4,  $t > 2.0$ ,  $P < 0.05$ ). These behavioural findings, though preliminary, are consistent with the hypothesis that rivalry dominance depends upon the ratio of monocular neurons activated by each eye<sup>3</sup>.

We calculated fMRI responses by averaging the fMRI time course surrounding all occurrences of a reported switch to the ipsilateral grating or blind-spot grating, time-locked to each reported switch. Figure 3 shows the average fMRI responses of each subject for rivalry versus stimulus alternation. The vertical bar at time zero indicates the time of the reported switch.

Although both gratings were constantly present during rivalry, the monocular blind-spot representation showed a sharp increase in fMRI activity soon after subjects reported that the ipsilateral grating had become perceptually dominant (Fig. 3a, green solid line). This rise in activity reflects the increased firing of the monocular neurons that receive input from the ipsilateral eye. Conversely, when the blind-spot grating became dominant, activity in this monocular region showed a sharp decrease (Fig. 3a, red dotted line). Thus, the signals from the ipsilateral eye to the V1 blind-spot representation were suppressed when the stimulus entering the other eye became perceptually dominant.

All four subjects showed the same qualitative pattern of awareness-related responses during rivalry. This tight correspondence between visual awareness and neural activity in monocular visual cortex confirms the predictions of interocular rivalry.

Functional MRI responses evoked by stimulus alternation (Fig. 3b) were remarkably similar to those observed during rivalry in their pattern, magnitude and timing. The initial peak or trough of the response always occurred from 0 to 2 s after the reported switch and the final peak or trough always occurred between 3 and 6 s after the switch. These peak-to-trough differences were highly reliable, yielding statistically significant linear or quadratic trends in fMRI responses within this time window (0 to 6 s) for all subjects, switch types and conditions ( $F > 4.1$ ,  $P < 0.05$ ).

To assess whether rivalry was fully resolved in the monocular V1 blind-spot representation, we compared the amplitude of fMRI responses (final minus initial peak-to-trough difference) for rivalry versus stimulus alternation. Figure 4 shows the normalized fMRI response amplitude of each subject, switch type and condition. Statistical analyses revealed that fMRI responses did not differ for

**Table 1 Perceptual dominance durations reported during rivalry**

Subject	Mean dominance duration (s)			Relative predominance (%)		
	Ipsilateral	Blind-spot	Blend	Ipsilateral	Blind-spot	Blend
S1	4.8	3.6	0.0	58	42	0
S2	2.9	2.3	0.7	55	41	4
S3	4.4	4.1	2.2	45	42	13
S4	6.1	2.8	1.4	65	29	6
Mean	4.6	3.2	1.1	56	38	6

Dominance durations for each grating followed a gamma-shaped distribution characteristic of binocular rivalry<sup>2</sup>; mean dominance durations are shown. Relative predominance is the percentage of total viewing time that the subject reported perceiving the ipsilateral grating only, the blind-spot grating only or a perceptual blend of both gratings.

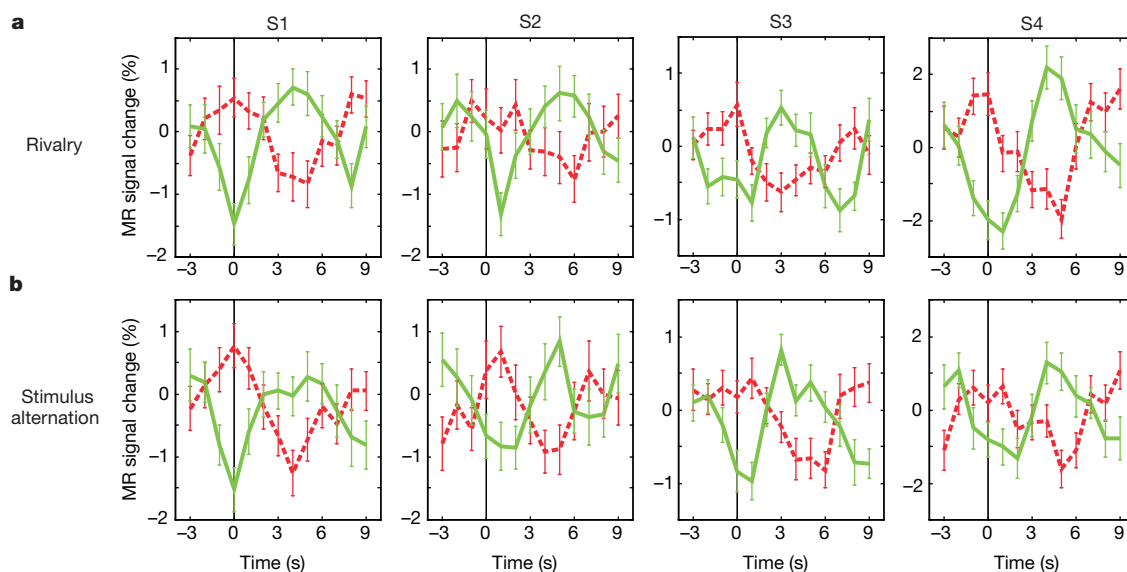


**Figure 3** fMRI activity during rivalry and stimulus alternation. Average fMRI activity in the V1 blind-spot representation during perceptual switches to the ipsilateral grating (green solid line) or blind-spot grating (red dotted line) for rivalry (**a**) versus stimulus alternation (**b**). Data of all four subjects are plotted on individually scaled y-axes. Vertical lines at time zero indicate the time of the subject's response. **a**, During rivalry, fMRI activity increases

sharply soon after the ipsilateral grating becomes dominant in awareness and decreases when the blind-spot grating becomes dominant, consistent with the predictions of interocular competition. **b**, Very similar fMRI responses occur during stimulus alternations between the two monocular gratings. (fMRI responses typically peak 2–6 s after stimulus onset because of haemodynamic lag.)

rivalry versus stimulus alternation ( $F < 1$ ). Positive responses for the ipsilateral grating were larger than negative responses for the blind-spot grating ( $F = 102, P < 0.005$ ) but rivalry and stimulus alternation remained equivalent across both types of neural response.

The equivalence between fMRI responses for rivalry and stimulus alternation indicates that it is likely that rivalry has been entirely resolved among monocular neurons in the V1 blind-spot representation, such that neural activity entirely reflects the subject's perceptual state. Thus, functionally equivalent neural responses are observed when the subject's conscious state alternates between the ipsilateral grating and blind-spot grating during constant rivalrous stimulation and when the physical stimulus itself alternates between each grating shown alone.

Our results show that binocular rivalry is resolved in monocular visual cortex and provide physiological evidence to support interocular competition. These theories predict that left-eye versus right-eye inputs are alternately suppressed during rivalry because of lateral inhibition among monocular V1 neurons<sup>3</sup> or feedback inhibition from V1 to monocular layers of the lateral geniculate nucleus<sup>12</sup>. In contrast, theories of pattern competition propose that rivalry occurs among binocular pattern neurons at much higher levels of the visual pathway and not among monocular neurons<sup>4</sup>. Our findings therefore help to resolve the neural basis of binocular rivalry.

Previous studies have found evidence of rivalry-related neural activity but none has established the involvement of monocular neurons<sup>4-6,8,13-18</sup>. In a single-unit study in monkeys, only 3 out of 33 V1 neurons showed significant responses corresponding to conscious perception, suggesting that rivalry takes place at higher levels of the visual pathway<sup>4</sup>. However, reanalysis revealed that across this V1 population, responses during rivalry equalled one-third of the magnitude of stimulus alternation responses<sup>13</sup>. These results are more consistent with an fMRI study showing reliable rivalry responses in human V1 that were about half the magnitude of stimulus alternation responses<sup>13</sup>. (Unfortunately, this study could not isolate monocular responses.) The authors suggested many factors that might account for the stronger rivalry effects in human V1, including interspecies differences, the indirect nature of fMRI in estimating neural activity, and the effects of eye movements on single-unit recordings.

In our view, the present finding of equally powerful rivalry and

stimulus alternation responses strongly suggests that binocular rivalry is resolved in monocular visual cortex. Although fMRI provides an indirect estimate of neural activity, any factors that might inflate response amplitudes during rivalry would also do so during stimulus alternation. In contrast, certain factors may have diluted rivalry responses in previous studies. These include sub-optimal viewing conditions that lead to frequent perceptual blends, and variability in the accuracy or timing of subjects' perceptual report. Isolating factors that weaken rivalry responses is an important direction for future research.

Although competition among binocular pattern neurons alone cannot account for our findings, it remains possible that feedback signals from binocular neurons to monocular neurons might yield the interocular suppression that we observe. However, such a theory fails to explain why pattern competition should lead to selection at the monocular level. Furthermore, it remains unclear how feedback projections from binocular neurons might target a specific monocular channel. Given these difficulties, interocular competition provides the most compelling explanation for rivalry in monocular visual cortex.

Our data also address a debate regarding whether common or separate neural mechanisms underlie binocular rivalry and related phenomena involving pattern rivalry. For example, two low-contrast patterns presented to one eye can weakly rival with each other<sup>1,19</sup>. Moreover, one of two dichoptic patterns can maintain dominance even when the patterns are frequently swapped between eyes<sup>20,21</sup>. Such rivalry probably involves high-level pattern competition. One proposal is that pattern competition may generally account for binocular rivalry<sup>20,22</sup>. However, our results suggest that a separate mechanism of interocular competition entirely accounts for the binocular rivalry in our subjects.

Finally, our findings show that neurons can reflect conscious perception at a much earlier level of the visual pathway than previously thought<sup>4,23</sup>. These results have one of two implications. One possibility is that certain aspects of conscious vision begin to emerge at the very earliest stage of cortical processing among monocular V1 neurons. Alternatively, our findings may suggest a new role for V1 as the 'gatekeeper' of consciousness, a primary cortical region that can select which visual signals gain access to awareness. In either case, our study firmly establishes the importance of primary visual cortex in binocular rivalry and conscious vision. □

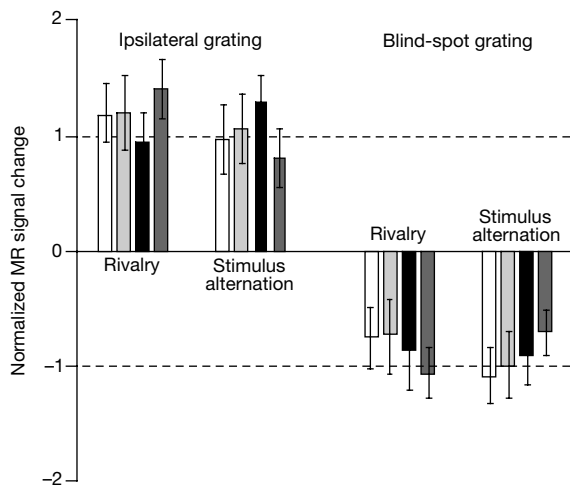


**Figure 4** fMRI response amplitudes for rivalry versus stimulus alternation. Amplitude of fMRI responses (peak-to-trough difference, time window 0 to +6 s) of each subject ( $n = 4$ ) for switches to the ipsilateral grating (left) and blind-spot grating (right) during rivalry versus stimulus alternation. Responses are normalized relative to each subject's mean response magnitude across the four conditions. fMRI responses for rivalry versus stimulus alternation did not reliably differ ( $F < 1$ ).

**Methods**

**Subjects**

Four healthy right-handed volunteers (three women), aged 21–28, participated. All had normal or corrected-to-normal visual acuity and normal stereo-depth perception. Two subjects were right-eye dominant and two were left-eye dominant. Before the fMRI experiment, subjects received training on how to localize their blind spot in visual space and to report their online perception during binocular rivalry and stimulus alternation.

**fMRI acquisition**

Subjects were scanned at the UCLA Division of Brain Mapping on a 3T General Electric scanner using a head coil. We collected functional images using 5–6 slices oriented perpendicular to the calcarine sulcus with the first slice beginning about 10 mm anterior to the occipital pole (slice thickness 4 mm, inter-slice distance 1 mm, in-plane resolution 3.125 × 3.125 mm). We used standard T2\*-weighted echoplanar imaging to localize the V1 blind-spot representation (TR = 2.5 s, TE = 45 ms, flip angle 80°) and for rivalry and stimulus alternation scans (TR = 1.0 s, TE = 45 ms, flip angle 45°). Functional images were superimposed on high-resolution T2-weighted anatomical images (in-plane resolution 0.78 × 0.78 mm). A bite bar minimized head motion.

**V1 blind-spot localization**

On separate fMRI scans, subjects viewed a counterphasing black/white checkerboard pattern with either their left ipsilateral eye or right blind-spot eye as shown in Fig. 1a. (In the actual experiment, a real fixation point was placed around 15° to the left of the subject's midline and the stimulus appeared roughly on the midline at a distance that closely corresponded to the subject's horopter.) Each scan consisted of an initial 30-s rest period followed by eight cycles of stimulation (15 s) and rest (15 s). We calculated activation maps and difference maps using multiple regression<sup>24</sup>. A linear model consisting of sinusoidal response functions was fit to the fMRI activity observed during the eight cycles of visual

stimulation for each eye. We identified the V1 blind-spot representation in individual subjects as those voxels in the left calcarine sulcus that showed both a significant response to ipsilateral stimulation and a significantly greater response to ipsilateral than blind-spot stimulation using a minimum statistical threshold of  $t = 2.0$ ,  $P < 0.05$ . The blind-spot representation ranged in size from 3–5 voxels (voxel size  $3.125 \times 3.125 \times 4$  mm) across subjects, consistent with size estimates based on post-mortem neuroanatomical studies (J. C. Horton, personal communication).

### Binocular rivalry and stimulus alternation scans

During these scans, two subjects viewed the red vertical grating and green horizontal grating with their left eye and right eye, respectively, whereas two subjects received the reverse eye assignment. Subjects performed 7–10 scans of rivalry and an equal number for stimulus alternation. Each scan lasted for 90 s. We discarded the first 10 s of fMRI activity to remove transient responses to the onset of the stimulus. We converted fMRI activity from the V1 blind-spot representation to per cent signal change from the mean level during the scan, and potential MR spikes and artefacts were minimized by reducing any outliers to lie within 3 s.d. of the mean.

We conducted an event-related fMRI analysis for reported switches between the blind-spot and ipsilateral grating. Previously, we found that rivalry responses increase as a function of percept duration and that very brief percepts led to unreliable fMRI responses<sup>8</sup>. Here, a switch was considered valid only if the percept immediately preceding and following the reported switch lasted longer than 2 s. An intervening blend response was allowed if it occurred within 1 s before the reported switch, in which case the blend duration was incorporated into the pre-switch period. fMRI responses of each subject were calculated by separately averaging the fMRI time course surrounding all occurrences of a reported switch to the ipsilateral grating or blind-spot grating for rivalry versus stimulus alternation, time-locked to each reported switch (rounded to the nearest second). Each average fMRI response function consisted of 39–55 observations.

Received 14 December 2000; accepted 12 February 2001.

- Helmholtz, H. v. *Helmholtz's Treatise on Physiological Optics* (The Optical Society of America, Rochester, New York, 1924).
- Levelt, W. J. M. *On Binocular Rivalry* (Royal VanGorcum, Assen, The Netherlands, 1965).
- Blake, R. A neural theory of binocular rivalry. *Psychol. Rev.* **96**, 145–167 (1989).
- Leopold, D. A. & Logothetis, N. K. Activity changes in early visual cortex reflect monkeys' percepts during binocular rivalry. *Nature* **379**, 549–553 (1996).
- Logothetis, N. K. & Schall, J. D. Neural correlates of subjective visual perception. *Science* **245**, 761–763 (1989).
- Sheinberg, D. L. & Logothetis, N. K. The role of temporal cortical areas in perceptual organization. *Proc. Natl Acad. Sci. USA* **94**, 3408–3413 (1997).
- Tootell, R. B. H. et al. Functional analysis of primary visual cortex (V1) in humans. *Proc. Natl Acad. Sci. USA* **95**, 811–817 (1998).
- Tong, F., Nakayama, K., Vaughan, J. T. & Kanwisher, N. Binocular rivalry and visual awareness in human extrastriate cortex. *Neuron* **21**, 753–759 (1998).
- Walls, G. L. The filling in process. *Am. J. Optom. Arch. Am. Acad. Optom.* **31**, 329–341 (1954).
- Stensaas, S. S., Eddington, D. K. & Dobbelle, W. H. The topography and variability of the primary visual cortex in man. *J. Neurosurg.* **40**, 747–755 (1974).
- Fox, R. & Rasche, F. Binocular rivalry and reciprocal inhibition. *Percept. Psychophys.* **5**, 215–217 (1969).
- Lehky, S. R. An astable multivibrator model of binocular rivalry. *Perception* **17**, 215–228 (1988).
- Polonsky, A., Blake, R., Braun, J. & Heeger, D. J. Neuronal activity in human primary visual cortex correlates with perception during binocular rivalry. *Nature Neurosci.* **3**, 1153–1159 (2000).
- Lansing, R. W. Electroencephalographic correlates of binocular rivalry in man. *Science* **146**, 1325–1327 (1964).
- Cobb, W. A., Morton, H. B. & Ettliger, G. Cerebral potential evoked by pattern reversal and their suppression in visual rivalry. *Nature* **216**, 1123–1125 (1967).
- Brown, R. J. & Norcia, A. M. A method for investigating binocular rivalry in real-time with the steady-state VEP. *Vision Res.* **37**, 2401–2408 (1997).
- Tononi, G., Srinivasan, R., Russell, D. P. & Edelman, G. M. Investigating neural correlates of conscious perception by frequency-tagged neuromagnetic responses. *Proc. Natl Acad. Sci. USA* **95**, 3198–3203 (1998).
- Lumer, E. D., Friston, K. J. & Rees, G. Neural correlates of perceptual rivalry in the human brain. *Science* **280**, 1930–1934 (1998).
- Wade, N. J. Monocular and binocular rivalry between contours. *Perception* **4**, 85–95 (1975).
- Logothetis, N. K., Leopold, D. A. & Sheinberg, D. L. What is rivalling during binocular rivalry? *Nature* **380**, 621–624 (1996).
- Lee, S. H. & Blake, R. Rival ideas about binocular rivalry. *Vision Res.* **39**, 1447–1454 (1999).
- Andrews, T. J. & Purves, D. Similarities in normal and binocularly rivalrous viewing. *Proc. Natl Acad. Sci. USA* **94**, 9905–9908 (1997).
- Crick, F. & Koch, C. Are we aware of neural activity in primary visual cortex? *Nature* **375**, 121–123 (1995).
- Friston, K. J. et al. Statistical parametric maps in functional imaging: A general linear approach. *Hum. Brain Mapp.* **2**, 189–210 (1994).

### Acknowledgements

We thank A. Seiffert and K. Nakayama for comments on this manuscript; D. Tran for research assistance; and J. Mazziotta, M. Cohen, the UCLA Brain Mapping Medical Organization, the Ahmanson Foundation, the Pierson-Lovelace Foundation, the Tamkin Foundation, and the Jennifer Jones-Simon Foundation for support. This research was funded by a McDonnell-Pew Grant in Cognitive Neuroscience and by the National Institutes of Health.

Correspondence and requests for materials should be addressed to F. T. (e-mail: ftong@princeton.edu).

## Linkage disequilibrium in the human genome

David E. Reich\*, Michele Cargill\*†, Stacey Bolk\*, James Ireland\*, Pardis C. Sabeti‡, Daniel J. Richter\*, Thomas Lavery\*, Rose Kouyoumjian\*, Shelli F. Farhadian\*, Ryk Ward‡ & Eric S. Lander\*§

\* Whitehead Institute / MIT Center for Genome Research, Nine Cambridge Center, Cambridge, Massachusetts 02142, USA

‡ Institute of Biological Anthropology, University of Oxford, Oxford OX2 6QS, UK

§ Department of Biology, MIT, Cambridge, Massachusetts 02139, USA

With the availability of a dense genome-wide map of single nucleotide polymorphisms (SNPs)<sup>1</sup>, a central issue in human genetics is whether it is now possible to use linkage disequilibrium (LD) to map genes that cause disease. LD refers to correlations among neighbouring alleles, reflecting 'haplotypes' descended from single, ancestral chromosomes. The size of LD blocks has been the subject of considerable debate. Computer simulations<sup>2</sup> and empirical data<sup>3</sup> have suggested that LD extends only a few kilobases (kb) around common SNPs, whereas other data have suggested that it can extend much further, in some cases greater than 100 kb<sup>4–6</sup>. It has been difficult to obtain a systematic picture of LD because past studies have been based on only a few (1–3) loci and different populations. Here, we report a large-scale experiment using a uniform protocol to examine 19 randomly selected genomic regions. LD in a United States population of north-European descent typically extends 60 kb from common alleles, implying that LD mapping is likely to be practical in this population. By contrast, LD in a Nigerian population extends markedly less far. The results illuminate human history, suggesting that LD in northern Europeans is shaped by a marked demographic event about 27,000–53,000 years ago.

To characterize LD systematically around genes, each of the 19 regions that we studied was anchored at a 'core' SNP in the coding region of a gene. The core SNP was chosen from a database of more than 3,000 coding SNPs that had been identified by screening in a multi-ethnic panel (see Methods), subject to two requirements. First, 'finished' genomic sequence was available for 160 kb in at least one direction from the core SNP; second, the frequency of the minor (less common) allele was at least 35% in the multi-ethnic panel.

We focused on high-frequency SNPs for several reasons. First, they tend to be of high frequency in all populations<sup>7</sup>, facilitating cross-population comparisons. Second, LD around common alleles represents a 'worst case' scenario: LD around rare alleles is expected to extend further because such alleles are generally young<sup>8</sup> and there has been less historical opportunity for recombination to break down ancestral haplotypes<sup>2</sup>. Third, LD around common alleles can be measured with a modest sample size of 80–100 chromosomes to a precision within 10–20% of the asymptotic limit (see Methods). Last, LD around common alleles will probably be particularly relevant to the search for genes predisposing to common disease<sup>9</sup>.

To identify SNPs at various distances from the core SNP, we re-sequenced subregions of around 2 kb centred at distances 0, 5, 10, 20, 40, 80 and 160 kb in one direction from the core SNP using 44 unrelated individuals from Utah. Altogether, we screened 251,310 bp (see Methods) and found an average heterozygosity of  $\pi = 0.00070$ , consistent with past studies<sup>1</sup>. A total of 272 'high frequency' polymorphisms were identified (Table 1).

We measured LD between two SNPs using the classical statistic  $D'$  (see Methods)<sup>10</sup>.  $D'$  has the same range of values regardless of the frequencies of the SNPs compared<sup>11</sup>. Its sign (positive or negative)

† Present address: Celera Genomics, 45 West Gude Drive, Rockville, Maryland 20850, USA.